THE ASTRONOMICAL JOURNAL, 119:840–850, 2000 February
© 2000. The American Astronomical Society. All rights reserved. Printed in U.S.A.

SPECTRAL COMPARISON OF RED GIANTS IN THE SECOND-PARAMETER GLOBULAR CLUSTER PAIR NGC 288 AND NGC 362

MATTHEW D. SHETRONE[1]
McDonald Observatory, University of Texas, P.O. Box 1337, Fort Davis, Texas 79734; shetrone@astro.as.utexas.edu
AND
MICHAEL J. KEANE[2]
Cerro Tololo Inter-American Observatory, Casilla 603, La Serena, Chile
Received 1999 September 24; accepted 1999 November 1

ABSTRACT

Abundances for 13 giants in the blue horizontal branch cluster NGC 288 and 12 giants in the red horizontal branch cluster NGC 362 are presented. The overall metallicities are found to be [Fe/H] = -1.39 ± 0.01 and -1.33 ± 0.01 for NGC 288 and NGC 362, respectively. [α/Fe] ratios for the two clusters are found to be nearly identical, although NGC 362 is found to have a 0.1 dex smaller [Ca/Fe] abundance. Contrary to previous investigations, oxygen-poor giants are found in both clusters. Although Na-O, Al-O anticorrelations are found in both clusters, zero-point and slope differences in the anticorrelations are found. These differences are attributed to ab initio higher O, Na, and Al abundances in NGC 288. Although the "mixed" giants in NGC 362 have significantly lower [O/Fe] ratios than those found in NGC 288, the extent of mixing is nearly equal in the two clusters because of this ab initio abundance difference. No significant difference is found in the *r*-process element Eu between the two clusters; however, the average Ba abundance, an *s*-process element, is slightly higher in NGC 288 than in NGC 362. Mass-loss indicators Hα and Na core velocities show little difference from previous investigations of other globular clusters. Excessive mass loss and deep mixing induced surface He abundance differences are ruled out as sources of the difference in horizontal-branch morphology for these two clusters.

Key words: globular clusters: individual (NGC 288, NGC 362) — stars: abundances — stars: mass loss

1. INTRODUCTION

If the number of reviews of a subject is an indication of its importance, then the second parameter problem of globular cluster horizontal branch morphology is very relevant (e.g., Fusi Pecci et al. 1996; Stetson et al. 1996; Peterson, Rood, & Crocker 1995; Catelan & de Freitas Pacheco 1996; Lee, Demarque, & Zinn 1994). The first parameter that affects the horizontal branch morphology in the globular cluster system is metallicity (Sandage & Wildey 1967; van den Bergh 1967). Age is another possible contributor to the morphology, but the range of age at any given metallicity within the globular cluster system is considered to be less than three billion years; thus, its contribution is much smaller than the overall metallicity affect. A list of the possible contributors to the second parameter affecting the horizontal branch morphology is just as long as the list of recent reviews: age, environmental concentration, primordial He abundance, postmixing surface He abundance, CNO abundance, rotation, and mass loss. Some of these candidates have well-founded theoretical standing but almost no observational evidence, e.g., primordial He abundance, postmixing surface He abundance, and mass loss, while some contributors, such as environmental concentration, have some observational evidence but little theoretical basis.

As an intermediate-mass giant evolves up the giant branch it is thought to lose mass. The amount of this mass loss can determine where the giant will eventually end up on the horizontal branch (D'Cruz et al. 1996). This mass loss can be measured, when strong enough, by mass-loss indicators such as the cores of strong lines or from emission in the wings, e.g., Mg II, Ca H and K, Na D, and Hα lines (Dupree, Hartman, & Avrett 1984). The Hα line is heavily affected by the chromospheric emission, which is related in some way to mass loss (Dupree & Smith 1995; Dupree et al. 1994; Smith & Dupree 1988). Thus the Hα line can exhibit both chromospheric emission in its wings and core shifts. The core shifts can be the result of line filling (in the case of strong emission) and/or outward-flowing material (Peterson 1981; Bates, Kemp, & Montgomery 1993; Kemp & Bates 1995; Lyons et al. 1996). The Na D lines are not affected by chromospheric emission, but the core of the lines are shifted toward the blue by outward-flowing mass (Peterson 1981; Bates et al. 1993; Shetrone 1994; Kemp & Bates 1995; Lyons et al. 1996). By combining information about core blueshifts with emission line strengths and line filling factors, we may make some assessment on the mass loss taking place within a globular cluster.

Recent high-resolution studies of abundances in globular cluster giants reveal an interesting property that separates clusters such as M10 and M13, which have very blue horizontal-branch stars (HBs), from a cluster like M3, which, at the same metallicity, has a "normal" red HB. First-ascent giants in M10 and M13, in contrast with M3 giants in the same evolutionary stage, show far more evidence for deep mixing of the envelope through the CNO-burning shell source (Kraft et al. 1992; Kraft et al. 1995).

[1] Visiting Astronomer, Cerro Tololo Inter-American Observatory. CTIO is operated by AURA, Inc., under contract to the National Science Foundation.
[2] Present address: Raytheon Systems Company, 100 Wooster Heights Road, Danbury, CT 06810.

This mixing succeeds in converting O to N in the envelope material. At the same time, the shell source mints fresh ^{23}Na and ^{27}Al by means of proton capture on ^{22}Ne and ^{24}Mg, ^{25}Mg, and ^{26}Mg, respectively, thus raising the abundances of these elements by more than an order of magnitude (Cavallo, Sweigart, & Bell 1998; Langer, Hoffman, & Zaidins 1997; Cavallo, Sweigart, & Bell 1996; Langer & Hoffman 1995). Of importance in the present context is that the same processing increases He at the expense of H, so that if mixing progresses as far as the observations of Al and Mg (Shetrone 1996b) indicate, the He/H ratio of HB progenitor giants in M13 might be raised by as much as 0.07 (i.e., from $Y = 0.23$ to 0.30). Such an increase in the He abundance would profoundly influence the HB morphology. An HB star with $\delta Y = +0.04$ would be moved from $T_{\rm eff} = 6000$ K to about 10,000 K (Rood 1973). The current understanding of the deep-mixing phenomenon suggests that Na is affected first, then O, Al, ^{26}Mg, ^{25}Mg, and, last, ^{24}Mg (Shetrone 1996b). Thus measuring the Al and Mg abundances within a cluster can suggest whether or not the surface He abundance has been altered.

This work addresses mass loss and light-element abundance as potential second parameter candidates in the globular clusters NGC 288 and NGC 362. NGC 288 has a blue HB [$(B-R)/(B+V+R) = 0.98$] and NGC 362 has a red HB [$(B-R)/(B+V+R) = -0.87$]. These globular clusters have been the subject of numerous abundance and photometric studies. Most analyses agree that the clusters have nearly the same metallicity, but the absolute value of that abundance is matter of contention. Estimates have ranged from [Fe/H] $= -0.9$ (Pilachowski & Sneden 1983) to [Fe/H] $= -1.4$ (Canterna, Ferrall, & Harris 1983; Costar & Smith 1988). Photometric studies also have been the center of controversy. Estimates of the age differences between the clusters have ranged from three billion years (Bolte 1989; Sarajedini & Demarque 1990) to zero billion years (Vandenberg & Durrell 1990; Stetson et al. 1996). We have obtained a large sample of spectra from giants in both clusters and analyzed them using well-founded techniques (the Lick-Texas scale, which includes clusters: M71, M5, M4, M3, M13, M15, M92, NGC 7006) to address the questions of [Fe/H], [α/Fe], degree of deep mixing, and strength of mass loss. This will help constrain the second-parameter candidates for these two clusters.

2. OBSERVATIONS

Table 1 displays the program stars, basic photometry, observation date and obtained signal-to-noise ratios. The program required the brightest likely members of the two clusters. For this reason, the samples were drawn from a number of sources. Older photometric surveys have lower quality photometry but cover the entire cluster, while more recent surveys usually cover only the outer regions of the cluster but have the most accurate photometry. For NGC 288, we have taken stars from Alcaino (1975); Olszewski, Canterna, & Harris (1984); and Frogel, Persson, & Cohen (1983). To compensate for zero-point difference between the photometric samples, we have added 0.09 mag to the V magnitudes of Alcaino (1975) but have not made any change to the colors. Most of the NGC 362 sample were drawn from Harris (1982). One bright giant (MB2) was added to the sample supplied by M. Bolte (1997, private communication). The coordinate position of MB2 corresponds to Tuc 215 (Tucholke 1992). Unfortunately, calibrated photometry was not available at the time for MB2. Values for reddening, $E(B-V)$, of 0.015 and 0.04 were adopted for NGC 288 and NGC 362 (Bolte 1989), respectively. NGC 362 has a much richer red giant tip than does NGC 288. This fact creates a color or temperature difference between the two samples of the cluster giants. Although there are 13 giants in the NGC 288 sample, only five giants in NGC 288 are in the temperature range of NGC 362. In addition to the program sample listed in Table 1, a series of rapidly rotating hot stars were observed at various air masses each night. These hot stars were used in the removal of telluric features from the program stars' spectra.

TABLE 1

PROGRAM STARS

Star	V	$(B-V)_0$	Date	S/N	References
		NGC 288			
531	12.9:	1.64:	1995 Oct 10	124	1, 4
403	12.92	1.47	1995 Oct 10	119	1
274	13.05	1.39	1995 Oct 10	106	1
20c.....	12.96	1.37	1995 Oct 10	91	1
281	13.27	1.26	1995 Oct 10	82	1
344	13.27	1.23	1996 Sep 26	72	1
245	13.45	1.25	1996 Sep 26	60	2
231	13.62	1.14	1996 Sep 26	58	2
338	13.63	1.13	1996 Sep 27	67	1
297	13.50	1.13	1996 Sep 27	74	2
351	13.54	1.14	1996 Sep 27	69	1
307	13.69	1.22	1996 Sep 27	59	2
287	13.66	1.23	1996 Sep 26	60	2
		NGC 362			
1401	12.63	1.53	1996 Sep 25	99	3
2115	12.58	1.64	1996 Sep 25	91	3
1423	12.60	1.56	1996 Sep 25	90	3
V2	12.7:	1.56:	1996 Sep 25	92	4
1334	12.83	1.48	1996 Sep 25	92	3
1441	12.72	1.59	1996 Sep 25	94	3
2423	12.80	1.61	1996 Sep 26	79	3
1137	12.78	1.41	1996 Sep 27	87	3
77.....	12.77	1.34	1996 Sep 27	95	3
MB2.....	...	...	1996 Sep 27	67	5
2127	12.89	1.50	1996 Sep 25	79	3
1159	12.68	1.36	1996 Sep 27	71	3

REFERENCES.—(1) photometry from Olszewski et al. 1984; (2) photometry from Alcaino 1975 with +0.09 mag to V; (3) photometry from Harris 1982; (4) photometry uncertain Frogel et al. 1983; (5) NGC 362 MB2 from M. Bolte (1997, private communication).

Observations were conducted at Cerro Tololo Inter-American Observatory using the 4 m Blanco telescope with the echelle spectrograph and the long focal length camera. The resulting spectra have a three pixel resolution of $R = 30{,}000$. Overscan, bias and dark removal, flat-field correction, scattered light removal, sky subtraction, extraction, and wavelength calibration were done in the standard IRAF NOAO.IMRED.ECHELLE package. Table 1 lists the signal-to-noise ratio per pixel at 6700 Å in the resulting spectra.

3. ANALYSIS

Equivalent widths were measured by fitting a Gaussian profile to the observed spectra lines using the IRAF SPLOT task. In the case of blended lines, several Gaussian profiles

TABLE 2

EQUIVALENT WIDTHS FOR NGC 288 GIANTS

λ	χ	log gf	531	403	274	20c	281	344	245	231	338	297	351	287	307
						O I									
6300.31.....	0.00	−9.75	91	78	67	38	76	44	45	40	50	35	22	34	28
6363.79.....	0.02	−10.25	67	28	36	16	25	18	26	24	16	11	13	18	14
						Na I									
6154.23.....	2.10	−1.56	39	28	...	53	17	40	20	20	...	26	37	31	26
6160.75.....	2.10	−1.26	63	43	34	76	20	45	25	22	24	53	65	43	40
						Mg I									
5528.41.....	4.35	−0.36	219	221	225	204	197	197	192	167	189	178	190	177	173
5711.09.....	4.35	−1.73	115	126	121	118	119	96	97	102	95	107	103	90	101
7387.69.....	5.75	−1.10	31	35	39	39	31	33	34	33	24	32	29	20	21
7691.55.....	5.75	−0.80	73	78	64	48	50	45	55	45	56	70	67	43	30
						Al I									
6696.03.....	3.14	−1.57	77	51	37	58	37	39	30	32	22	31	37	35	45
6698.67.....	3.14	−1.89	45	30	22	35	20	19	12	15	8	16	25	24	17
7835.31.....	4.02	−0.71	...	...	...	...	...	20	...	...	...	...	29	...	18
7836.13.....	4.02	−0.55	...	...	...	...	...	30	...	...	...	27	32	30	30
						Si I									
6142.49.....	5.62	−1.48	...	...	25	...	...	18	28	25	22	...	...	...	...
6145.02.....	5.61	−1.37	...	...	...	35	19	17	26	...	17	...	...	19	...
6243.82.....	5.61	−1.27	...	25	31	27	23	42	22	23	28	25	19	19	21
6244.48.....	5.61	−1.27	...	18	24	20	...	18	19	26	23	21	22	25	17
						Ca I									
6161.30.....	2.52	−1.27	104	111	115	105	87	80	75	79	79	69	75	57	60
6166.44.....	2.52	−1.14	95	107	110	95	88	88	76	80	76	73	79	78	68
6169.04.....	2.52	−0.80	132	131	131	112	114	110	103	99	91	110	102	93	83
6169.56.....	2.52	−0.48	148	149	148	127	119	127	110	113	115	121	117	91	114
6439.08.....	2.52	0.39	192	200	186	182	179	174	167	153	161	160	166	152	153
6455.60.....	2.52	−1.29	99	94	84	95	79	67	72	65	63	67	66	67	66
6499.65.....	2.52	−0.82	135	134	126	110	97	99	99	103	85	94	94	85	83
						Sc II									
6279.74.....	1.50	−1.16	...	59	...	60	...	58	49	57	50	46	41	48	37
6309.90.....	1.50	−1.52	55	40	46	31	46	35	36	...	36	34	23	28	...
						Ti I									
6303.77.....	1.44	−1.57	95	73	67	59	47	43	30	...	28	33	31	31	...
6312.24.....	1.46	−1.55	106	77	66	49	50	45	37	28	38	37	33	...	17
						V I									
6216.37.....	0.28	−1.07	184	161	147	140	129	106	89	70	...	74	84	69	60
6224.51.....	0.29	−1.82	110	109	91	87	72	75	41	51	43	40	46	28	...
6233.20.....	0.28	−2.00	167	96	79	61	61	48	30	27	29	35	33	...	20
6274.66.....	0.27	−1.69	150	119	103	88	76	73	55	50	49	42	49	36	47
6285.16.....	0.28	−1.56	150	124	110	93	95	79	63	41	60	50	48	46	48
6292.82.....	0.29	−1.52	193	134	110	97	75	82	57	61	60	55	59	53	50
6452.31.....	0.29	−1.21	91	55	41	34	30	...	...	23	...	...	...	...	...
6504.19.....	1.18	−1.23	74	47	31	32	46	24	...	...	...	33	...	...	...
						Fe I									
6151.62.....	2.18	−3.37	114	113	108	105	94	96	85	86	80	93	81	68	79
6157.73.....	4.07	−1.26	86	79	83	75	83	69	63	57	62	56	69	52	56
6165.36.....	4.14	−1.47	49	48	56	37	37	36	22	40	29	30	37	25	35
6213.43.....	2.22	−2.66	135	162	150	134	136	134	123	113	114	115	120	95	106
6219.28.....	2.20	−2.44	134	163	161	139	144	148	122	122	126	122	124	110	107
6226.74.....	3.88	−2.22	49	38	37	30	23	24	34	27	24	27	24	...	...
6229.23.....	2.84	−3.00	112	73	81	62	69	53	35	41	62	52	55	43	...
6240.66.....	2.22	−3.23	96	109	111	105	100	94	76	70	75	81	78	63	81
6280.62.....	0.86	−4.37	163	190	167	168	154	156	143	122	132	136	131	116	121

TABLE 2—*Continued*

λ	χ	log *gf*	531	403	274	20c	281	344	245	231	338	297	351	287	307
6290.97.....	4.73	−0.76	...	42	41	32	34	46	29	36	33	28	30	38	34
6297.80.....	2.22	−2.74	139	147	156	128	128	109	95	110	116	121	117	93	97
6301.50.....	3.65	−0.72	102	124	124	113	126	116	104	109	110	109	99	94	104
6302.49.....	3.69	−1.15	85	100	93	92	97	89	88	84	98	82	77	83	85
6311.51.....	2.83	−3.22	89	62	56	48	60	53	39	29	41	42	50	25	25
6355.04.....	2.84	−2.29	107	125	120	117	101	114	98	98	88	99	104	78	91
6380.75.....	4.19	−1.40	74	50	53	60	50	49	42	31	41	40	53	45	31
6419.96.....	4.73	−0.24	75	71	72	76	58	60	63	54	66	62	69	59	54
6421.35.....	2.28	−1.94	203	...	179	173	169	156	...	151	146	148	148	153	142
6430.85.....	2.18	−2.00	191	212	204	188	189	178	...	153	150	161	158	160	134
6498.94.....	0.96	−4.69	187	158	151	143	121	122	106	121	104	110	106	95	83
6574.23.....	0.99	−5.02	148	136	130	118	104	101	85	78	80	87	78	72	72
							Fe II								
6149.25.....	3.89	−2.72	...	...	19	...	18	21	37	...	...	18	...	...	19
6369.46.....	2.89	−4.25	...	...	...	...	17	...	...	...	...	...	...	...	...
6416.93.....	3.89	−2.79	...	22	...	17	19	29	18	25	...	26	26	...	17
6432.68.....	2.89	−3.71	20	35	30	28	41	38	29	32	38	28	31	39	35
6456.39.....	3.90	−2.08	39	40	43	48	54	43	39	44	41	51	...	38	53
6516.08.....	2.89	−3.45	...	47	42	36	43	54	53	42	43	45	52	46	31
							Ni I								
6175.37.....	4.09	−0.53	52	42	36	35	30	36	36	26	25	30	27	28	31
6176.82.....	4.09	−0.53	48	57	55	46	44	50	...	44	45	42	38	43	48
6177.25.....	1.83	−3.50	68	54	60	42	33	38	36	26	21	30	28	29	18
6223.99.....	4.10	−0.99	...	...	...	...	...	...	...	...	...	...	...	...	...
6378.26.....	4.15	−0.89	...	19	19	...	...	17	18	22	...	29	...	...	...
							Ba II								
5853.69.....	0.60	−1.01	127	150	148	139	127	125	124	113	123	118	111	113	114
6141.73.....	0.70	−0.08	192	222	222	203	186	183	175	168	177	166	175	163	171
6496.91.....	0.60	−0.38	222	216	210	201	184	185	173	167	180	173	168	168	158
							Eu II								
6645.13.....	1.37	0.20	38	37	37	35	35	37	35	39	24	29	24	32	27

with fixed FWHM were fitted to the observed spectra. In regions where telluric features contaminated the stellar spectra, division by a hot star with the appropriate line depth was made to remove these lines. If a spectral line happened to fall on a bad column or cosmic ray hit, the line was not included in this analysis. The equivalent widths are listed in Tables 2 and 3.

Initial estimates for effective temperature, $T_{\rm eff}$, and surface gravity, log g, were made from optical colors (see Table 1 for references), infrared colors from Frogel et al. (1983), and temperature-sensitive line-depth ratios in the manner of Gray (1994). We use our own calibration of the values of $(B-V)$ to $T_{\rm eff}$ and surface gravity for red giants with [Fe/H] metallicities of -1.0 to -1.5. We adopt the Ridgway et al. (1980) conversion from $(V-K)_0$ to effective temperature. The line-depth method employs temperature-sensitive and temperature-insensitive spectral lines to determine effective temperatures. We found good results employing the Gray 1994 temperature-sensitive V I lines d5 λ6224.5, d8 λ6233.2, d13 λ6251.8, and d15 λ6256.9 measured with respect to the temperature-insensitive Fe I lines d7 λ6229.2 and d14 λ6252.6. To determine the slope and zero point of the line-depth calibration, we used the average color temperature. The brightest giants in globular clusters are known to be long period variables (e.g., NGC 362 V2 and NGC 288 531). Because our sample of giants was taken from the brightest giants within the two clusters, the temperature based on colors will, in some cases, be inaccurate and thus the line-depth temperatures are very valuable. The rms scatter between the different temperature estimates is 45 K.

The initial estimates of the effective temperature and surface gravity were "fine-tuned" using the numerous Fe I and Fe II lines from the high-resolution spectra. These Fe lines are the same ones used by the Lick-Texas group (see Kraft et al. 1995). A final model was developed by demanding the simultaneous conditions of no slope in plots of Fe abundance (from Fe I) versus both excitation potential and equivalent width and enforcing ionization equilibrium, such that both Fe I and Fe II yield the same abundance. The microturbulent velocity was allowed to vary to remove any slope of the Fe I abundance versus equivalent width. The "fine-tuned" stellar parameters do not vary significantly from the initial estimates. The largest difference in effective temperature, 75 K, is found in NGC 362 V2, 2127, 1441 and NGC 288 531. The largest difference in surface gravity, 0.3 dex, is found in NGC 362 77. We adopt the "fine-tuned" stellar parameters but would not get significantly different results from adopting the initial estimates. The adopted stellar parameters are listed in Table 4.

We adopt the lines and atomic parameters from the Lick-Texas group (Sneden et al. 1991; Kraft et al. 1993;Armosky et al. 1994; Kraft et al. 1995; Shetrone 1996a). The lines and equivalent widths are listed in Tables 2 and 3. In addition to

TABLE 3

EQUIVALENT WIDTHS FOR NGC 362 GIANTS

λ	χ	log gf	1401	2115	1423	V2	1334	1441	2423	1137	77	MB2	2127	1159
						O I								
6300.31.....	0.00	−9.75	76	81	63	100	74	56	51	61	30	48	45	68
6363.79.....	0.02	−10.25	40	41	25	47	36	24	17	30	16	19	...	35
						Na I								
6154.23.....	2.10	−1.56	27	20	40	...	21	34	30	25	36	49	32	22
6160.75.....	2.10	−1.26	56	35	55	...	31	49	55	32	60	79	61	33
						Mg I								
5528.41.....	4.35	−0.36	220	227	230	291	220	218	203	245	262	241	217	188
5711.09.....	4.35	−1.73	127	130	126	140	105	122	117	131	137	118	112	125
7387.69.....	5.75	−1.10	32	29	35	40	44	35	30	36	25	18	25	27
7691.55.....	5.75	−0.80	62	63	75	83	63	66	63	55	68	50	56	56
						Al I								
6696.03.....	3.14	−1.57	32	27	75	40	27	43	58	22	77	49	57	20
6698.67.....	3.14	−1.89	17	19	46	...	...	27	31	19	39	28	28	21
7835.31.....	4.02	−0.71	25	...	30	20	...	27	22	...	50	26	40	...
7836.13.....	4.02	−0.55	32	25	36	28	30	40	49	...	64	28	54	...
						Si I								
6142.49.....	5.62	−1.48	22	...	...	...	...	...	...	...	...	...	...	...
6145.02.....	5.61	−1.37	...	...	...	...	...	...	...	20	...	...	...	...
6243.82.....	5.61	−1.27	...	...	27	...	21	28	...	20	30	...	18	...
6244.48.....	5.61	−1.27	...	...	26	...	...	18	...	...	33	25	27	...
						Ca I								
6161.30.....	2.52	−1.27	110	104	110	76	117	105	106	100	114	102	99	100
6166.44.....	2.52	−1.14	114	110	108	124	110	107	112	100	113	115	98	106
6169.04.....	2.52	−0.80	132	149	159	165	123	129	130	127	140	142	128	127
6169.56.....	2.52	−0.48	142	157	152	202	141	148	147	140	160	151	146	142
6439.08.....	2.52	0.39	207	210	221	273	204	203	191	185	241	210	197	186
6455.60.....	2.52	−1.29	97	104	97	111	98	96	88	90	96	94	88	91
6499.65.....	2.52	−0.82	142	138	140	143	143	134	122	126	131	127	125	120
						Sc II								
6279.74.....	1.50	−1.16	69	64	77	...	55	64	63	67	64	66	63	63
6309.90.....	1.50	−1.52	62	46	63	51	47	36	48	34	43	67	34	40
						Ti I								
6303.77.....	1.44	−1.57	95	99	89	116	81	73	83	73	73	72	64	73
6312.24.....	1.46	−1.55	95	86	100	97	82	71	66	63	64	80	54	71
						V I								
6216.37.....	0.28	−1.07	188	177	180	155	168	159	154	155	160	159	135	134
6224.51.....	0.29	−1.82	125	112	110	67	102	103	89	92	92	87	75	89
6233.20.....	0.28	−2.00	119	118	106	122	93	96	83	91	83	89	69	77
6274.66.....	0.27	−1.69	150	137	135	132	120	115	113	110	107	100	100	97
6285.16.....	0.28	−1.56	151	152	141	158	133	130	122	119	121	113	105	97
6292.82.....	0.29	−1.52	166	166	162	134	138	120	125	120	127	136	105	104
6452.31.....	0.29	−1.21	82	59	59	55	55	52	46	43	43	41	32	33
6504.19.....	1.18	−1.23	63	48	45	35	43	45	41	46	41	43	30	40
						Fe I								
6151.62.....	2.18	−3.37	125	148	128	148	124	125	102	113	130	127	122	107
6157.73.....	4.07	−1.26	97	83	100	95	98	94	94	90	89	102	92	85
6165.36.....	4.14	−1.47	48	52	44	...	42	54	52	53	60	52	49	53
6213.43.....	2.22	−2.66	155	179	182	200	158	170	156	151	178	205	168	151
6219.28.....	2.20	−2.44	176	194	192	176	178	176	168	162	194	165	182	162
6226.74.....	3.88	−2.22	49	45	37	58	41	41	31	24	38	34	32	38
6229.23.....	2.84	−3.00	82	93	76	100	88	73	76	66	90	80	75	75
6240.66.....	2.22	−3.23	115	144	121	153	115	120	113	114	147	117	121	108
6280.62.....	0.86	−4.37	204	222	231	260	197	188	189	191	223	227	197	172

TABLE 3—*Continued*

λ	χ	log *gf*	1401	2115	1423	V2	1334	1441	2423	1137	77	MB2	2127	1159
6290.97.....	4.73	−0.76	56	52	55	...	55	53	47	43	56	54	46	...
6297.80.....	2.22	−2.74	151	168	172	164	146	153	145	135	166	173	164	154
6301.50.....	3.65	−0.72	126	147	145	202	131	136	145	128	154	138	168	131
6302.49.....	3.69	−1.15	104	123	129	126	110	108	111	110	123	103	121	108
6311.51.....	2.83	−3.22	87	93	91	72	79	77	75	58	...	75	59	72
6355.04.....	2.84	−2.29	136	136	140	157	138	131	123	127	155	142	135	125
6380.75.....	4.19	−1.40	61	63	59	75	60	61	59	64	61	66	62	58
6419.96.....	4.73	−0.24	80	85	90	108	80	78	83	84	90	100	93	80
6421.35.....	2.28	−1.94	198	222	236	256	201	189	189	198	228	217	...	181
6430.85.....	2.18	−2.00	225	243	240	265	210	211	199	200	253	237	215	200
6498.94.....	0.96	−4.69	183	185	200	272	170	161	153	165	197	199	166	142
6574.23.....	0.99	−5.02	151	169	180	203	138	136	127	137	159	165	137	115
						Fe II								
6149.25.....	3.89	−2.72	31	...	28	...	18	24	28	...	35	17	...	25
6369.46.....	2.89	−4.25	20	17	25	32	17	21	21	...	25	38	...	19
6416.93.....	3.89	−2.79	33	27	24	...	31	26	23	...	...	20	25	22
6432.68.....	2.89	−3.71	44	40	34	43	38	38	37	20	53	46	42	35
6456.39.....	3.90	−2.08	40	46	65	88	52	53	41	53	76	69	66	48
6516.08.....	2.89	−3.45	40	62	53	46	56	50	58	45	71	65	57	48
						Ni I								
6175.37.....	4.09	−0.53	33	36	34	...	38	36	36	37	44	44	32	32
6176.82.....	4.09	−0.53	59	57	57	47	45	57	63	54	62	60	53	55
6177.25.....	1.83	−3.50	60	64	71	53	55	56	54	50	59	52	49	53
6223.99.....	4.10	−0.99	25	21	19	...	18	20	18	16	...	...	...	...
6378.26.....	4.15	−0.89	23	26	25	...	24	19	...	28	24	20	22	...
						Ba II								
5853.69.....	0.60	−1.01	151	164	167	220	152	151	135	140	190	201	152	140
6141.73.....	0.70	−0.08	219	229	260	339	209	217	205	203	274	283	249	192
6496.91.....	0.60	−0.38	210	218	248	370	213	203	197	198	290	282	223	179
						Eu II								
6645.13.....	1.37	0.20	60	56	53	68	47	49	53	49	58	44	54	50

an abundance analysis of the equivalent widths, we determined the abundance of some lines based on synthetic spectra. The region around the λ6300 [O I] line and the region around the λλ5682, 5688 Na I doublet are crowded and require synthetic spectra. The abundances for O and Na are based on the abundances derived by both synthetic and equivalent-width analyses. Although the equivalent widths for eight V I lines are given in Tables 2 and 3, only two lines, λλ6285 and 6274, were used in the abundance analysis. Hyperfine structure is available for these two lines from McWilliam & Rich (1994). The derived abundances for the program stars are listed in Table 4.

4. DISCUSSION

4.1. *The Abundances*

The overall abundance we find for NGC 288 and NGC 362 is [Fe/H] = -1.39 ± 0.01 and -1.33 ± 0.01, respectively. Figure 1 displays the even Z elements not affected by moderate amounts of deep mixing plotted against $T_{\rm eff}$. Within the errors, there are no significant trends with temperature. The overall even Z abundance is enhanced with respect to iron, as is seen in most metal-poor giants. The average Si, Ti, and Mg abundances are consistent between the two clusters. However, the Ca abundance is slightly lower, 0.1 dex, in NGC 362 than in NGC 288. This is not unusual since many clusters exhibit different average abundances for these even Z elements.

In Figure 2, the Na and Al abundances are plotted against the O abundances. Both NGC 362 and NGC 288 exhibit clear evidence of an Na-O anticorrelation. However, these anticorrelations do not exhibit the same slope or intercept. At a given O abundance, NGC 288 has a higher Na abundance than does NGC 362. In addition, the slope of the NGC 288 Na-O anticorrelation is steeper than the NGC 362 anticorrelation. If we take the stars with the highest O abundances and lowest Na abundances as completely chemically unevolved (as far as deep mixing is concerned), then we would say that NGC 362 has both a lower ab initio O and Na abundance than does NGC 288. This is not unprecedented since NGC 362 also has a lower Ca abundance. If the NeNa reaction rates assumed in Langer et al. (1997) and adopted in Shetrone (1996b) are correct (these reaction rates are very uncertain), then it would be difficult to assume that the two clusters did start with the same ab initio Na and O abundances. The deep-mixing hierarchy (see Shetrone 1996b) is such that we expect Ne-Na conversion before O-N conversion. We cannot expect significant O depletion without having significant Na enhancement. However, it would be possible that the clusters had the same ab initio O abundances but different Na abundances.

NGC 362 exhibits clear evidence for a Al-O anticorrelation while NGC 288 exhibits only marginal evidence (1 σ). The same zero-point offset seen in the Na-O anti-

TABLE 4

ABUNDANCES FOR PROGRAM STARS

Star	T	g	v_t	Fe	O	Na	Mg	Al	Si	Ca	Sc	Ti	V	Ni	Ba	Eu
							NGC 288									
531	3780	0.10	1.60	−1.31	0.38	0.00	0.46	0.59	...	0.09	0.13	0.25	−0.04	0.10	0.23	0.34
403	3950	0.20	1.90	−1.43	0.19	0.08	0.59	0.53	0.38	0.32	−0.10	0.29	0.00	0.03	0.39	0.39
274	4025	0.70	1.90	−1.37	0.37	−0.05	0.47	0.33	0.56	0.29	0.13	0.28	−0.01	0.06	0.44	0.51
20c.....	4050	0.60	1.75	−1.44	−0.02	0.60	0.48	0.72	0.58	0.29	−0.03	0.23	−0.07	0.00	0.44	0.52
281	4125	0.60	1.71	−1.42	0.35	−0.09	0.46	0.45	0.39	0.25	0.15	0.28	0.04	−0.09	0.29	0.50
344	4180	0.80	1.60	−1.36	0.09	0.32	0.32	0.40	0.41	0.25	−0.01	0.25	0.00	−0.01	0.37	0.56
245	4250	0.80	1.40	−1.41	0.27	0.02	0.49	0.35	0.47	0.39	−0.02	0.27	0.03	0.01	0.53	0.59
231	4300	1.10	1.50	−1.41	0.34	0.03	0.38	0.45	0.52	0.36	0.16	0.24	−0.07	0.04	0.40	0.77
338	4325	1.30	1.60	−1.37	0.35	−0.06	0.34	0.16	0.44	0.23	0.12	0.32	0.07	−0.08	0.49	0.46
297	4330	1.20	1.70	−1.41	0.15	0.38	0.48	0.46	0.40	0.30	0.04	0.39	−0.02	0.11	0.31	0.57
351	4330	1.20	1.55	−1.33	−0.02	0.54	0.48	0.55	0.26	0.28	−0.18	0.27	−0.05	−0.10	0.33	0.38
307	4350	1.20	1.35	−1.40	0.15	0.34	0.30	0.55	0.29	0.29	−0.16	0.04	0.07	0.02	0.54	0.55
287	4350	1.20	1.40	−1.45	0.25	0.46	0.35	0.66	0.41	0.33	0.02	0.43	0.03	0.08	0.48	0.66
							NGC 362									
1401	3875	0.00	1.90	−1.32	0.08	−0.08	0.41	0.17	0.54	0.16	0.00	0.29	0.04	−0.07	0.18	0.62
2115	3900	0.00	2.30	−1.38	0.16	−0.13	0.38	0.14	...	0.11	−0.18	0.31	−0.05	−0.01	0.00	0.53
1423	3950	0.10	2.35	−1.37	−0.04	0.20	0.42	0.47	0.41	0.17	0.03	0.38	−0.02	−0.05	0.26	0.50
V2	3950	0.10	2.70	−1.30	0.21	−0.20	0.48	0.18	...	0.13	−0.15	0.36	−0.10	−0.23	0.73	0.58
1334	3975	0.40	1.95	−1.30	0.18	−0.20	0.33	0.13	0.25	0.20	−0.15	0.27	−0.02	−0.11	0.22	0.50
1441	3975	0.20	1.90	−1.31	−0.09	0.09	0.41	0.37	0.28	0.23	−0.23	0.19	−0.05	−0.11	0.20	0.48
2423	4000	0.40	1.85	−1.32	−0.11	0.16	0.33	0.47	...	0.23	−0.05	0.28	−0.02	−0.04	0.15	0.64
1137	4000	0.70	2.00	−1.37	0.25	−0.15	0.48	0.02	0.39	0.13	0.01	0.21	−0.02	0.02	0.19	0.72
77.....	4075	0.20	2.50	−1.34	−0.33	0.28	0.44	0.78	0.42	0.25	−0.24	0.30	0.00	−0.02	0.47	0.53
MB2.....	4100	0.60	2.50	−1.33	−0.01	0.40	0.19	0.40	0.32	0.14	0.07	0.39	−0.03	−0.03	0.63	0.47
2127	4110	0.60	2.25	−1.30	−0.09	0.20	0.21	0.58	0.23	0.12	−0.19	0.21	−0.03	−0.11	0.24	0.62
1159	4125	0.80	1.90	−1.27	0.31	−0.13	0.25	0.01	...	0.24	−0.04	0.41	−0.02	−0.05	0.10	0.67

correlation is also exhibited in the Al-O anticorrelation: at a given O abundance, NGC 288 has a higher Al abundance than does NGC 362. If we assume that the stars with the largest O abundance are unmixed (as far as deep mixing is concerned), then we would say that NGC 362 has both a lower ab initio O and Al abundance. The deep-mixing hierarchy states that one does not expect Al enhancements to take place without O being enhanced. Thus, to produce a significant Al enhancement would require some O depletion and, therefore, the two clusters cannot have begun with the same ab initio Al and O abundances. Thus, based on the Na-O and Al-O anticorrelations, we conclude that NGC 288 has an ab initio higher Na, Al, and O abundance than does NGC 362 by 0.15 dex.

Figure 3 exhibits the Na and Mg abundances plotted with respect to the Al abundance. There is a positive correlation between Na and Al but no correlation between Mg and Al in both clusters. This is not a surprise based on the small size of the Al enhancements and O depletions. According to the deep-mixing hierarchy, only when the O depletions and Al enhancements are extreme, $[O/Fe] < -0.4$ and $[Al/Fe] > 0.9$, is the Al-Mg anticorrelation detectable in the overall Mg abundance. The Mg isotopes ^{25}Mg ^{26}Mg can be turned into Al during proton capture, but the more abundant ^{24}Mg can be turned into Al only at the highest temperatures and, hence, during the most extreme deep mixing. Typical Mg isotope ratios for metal-poor halo stars are 88:6:6 for ^{24}Mg:^{25}Mg:^{26}Mg (Barbuy, Spite, & Spite 1987; McWilliam & Lambert 1988; Shetrone 1996b). If we assume that the ab initio Al abundance is higher in NGC 288 than in NGC 362, then we expect 0.55 and 0.30 dex enhancements in Al for NGC 362 and NGC 288, respectively, if all of the surface ^{25}Mg and ^{26}Mg atoms are converted to Al. This would decrease the overall Mg abundance by 0.06 dex, which may not be detectable in our current sample size and errors. As can be seen in Figure 3, Al enhancements of 0.4 and 0.2 dex are observed in NGC 362 and NGC 288. Thus we conclude that the Al abundances seen in NGC 288 and NGC 362 are fully consistent with Al enhancement from ^{25}Mg and ^{26}Mg.

Figure 4 exhibits the Eu and Ba abundances for our sample. The Eu abundances of NGC 288 and NGC 362 are equal within the errors, but the Ba abundances of NGC 362 are slightly lower (1 σ) than those found in NGC 288. We should point out that Ba II lines are quite strong and formed at small optical depths and are therefore sensitive to chromospheric activity. The two giants in NGC 362 that exhibit the greatest chromospheric activity also exhibit the largest Ba abundance. We suggest that, for these two giants, our Ba II estimates are probably being adversely affected by chromospheric affects we are unable to model.

4.2. *Comparison to Other Analyses*

Pilachowski & Sneden (1983) was one of the first high-resolution surveys of NGC 362. We share two stars in common with their sample of three NGC 362 giants. A comparison of the equivalent widths reveals a factor of 2 difference between the Pilachowski & Sneden (1983) widths and those presented in this work. It is not surprising that Pilachowski et al. found abundances much larger than those reported in this work by more than a factor of 0.4 dex. We suggest that this difference is probably caused by the difficulty of working with image tube spectra recorded on glass plates.

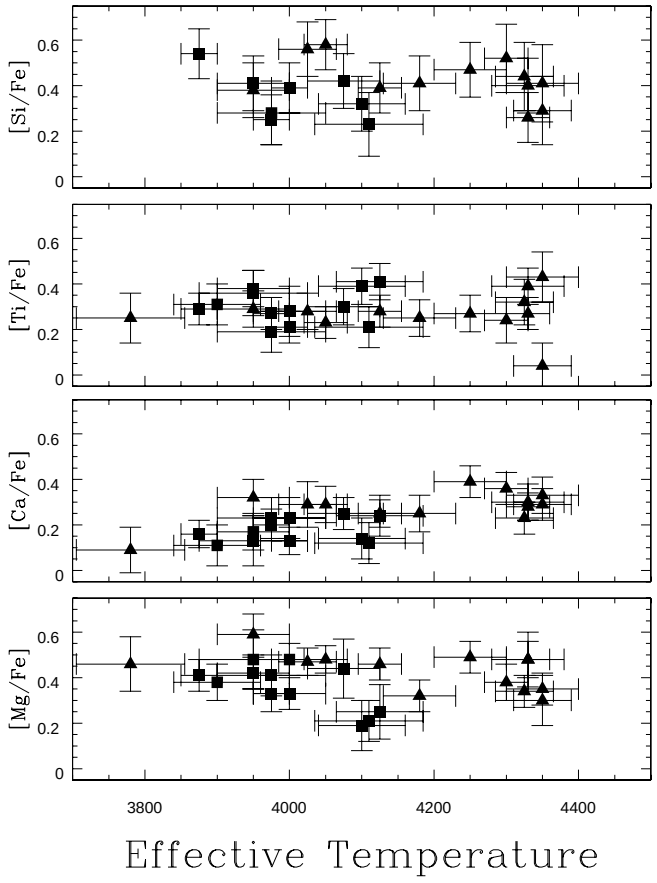


FIG. 1.—Abundances of the elements not affected by moderate amounts of deep mixing plotted against the stars' effective temperatures. The triangles represent the NGC 288 sample and the squares represent the NGC 362 sample. Error bars represent 1 σ errors.

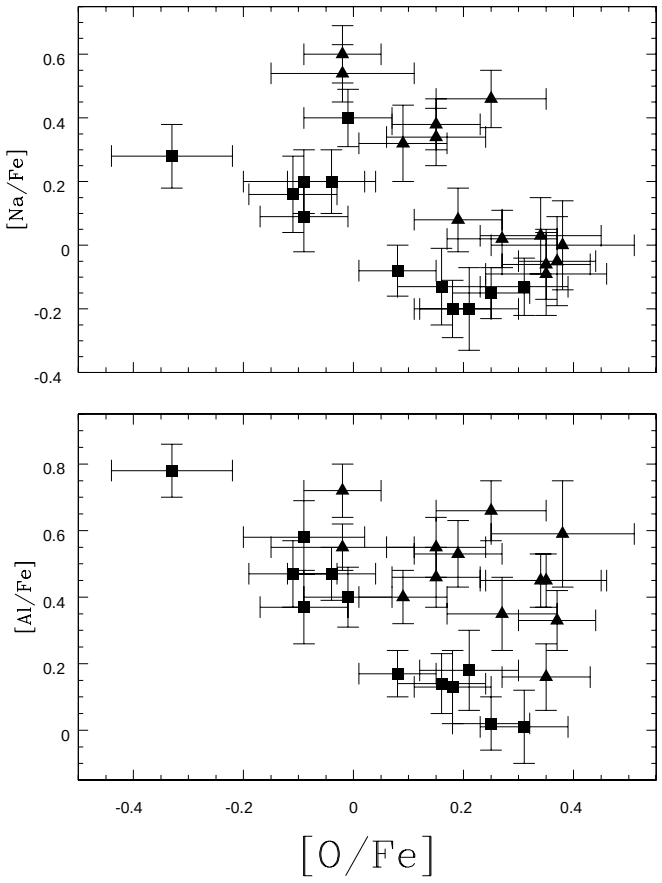


FIG. 2.—Abundances of the deep-mixing elements Al and Na are compared to the oxygen abundances. The triangles represent the NGC 288 sample and the squares represent the NGC 362 sample. Error bars represent 1 σ errors.

Gratton 1987 conducted an abundance analysis of a small sample of NGC 288 and NGC 362 stars, one star in NGC 362 and two stars in NGC 288. Our sample has the two NGC 288 stars in common with the Gratton sample. Our equivalent widths are found to be $\sim$20% smaller than those in Gratton 1987. Our $T_{\rm eff}$ are 160 K cooler than those found by Gratton. This temperature difference is largely because of the choice of temperature scales. Gratton did not make any correction for a slope of abundance versus excitation potential. Overall, his derived abundances are significantly smaller than those of Pilachowski & Sneden (1983) but somewhat higher ($\sim$0.1 dex) than those found in this work. This difference can be attributed easily to the lower resolution (15,000), lower signal-to-noise ratio (S/N $\sim$ 50) and smaller sample size of the Gratton sample.

Dickens et al. (1991) report on the abundances of nine NGC 362 stars and six NGC 288 stars. They find an overall abundance of [Fe/H] = -1.03 and -0.98 for NGC 288 and NGC 362, respectively. The equivalent widths measured in this sample agree remarkably well with those used in the Dickens et al. (1991) abundance analysis of both NGC 288 and NGC 362 (Croke 1992). For the eight stars in common with the Dickens NGC 362 sample, our temperatures are 45 K (σ = 64 K) cooler; for the single star in common with the Dickens NGC 288 sample, we derive a temperature 140 K cooler than Dickens (Croke 1992). Thus, given the similarities between the equivalent widths and effective temperatures, we assume that the abundance differences found between Dickens et al. (1991) and this survey are caused mostly by choices of oscillator strengths. Looking at differential abundances, the Dickens's sample and our sample yield very similar results for the stars the two samples have in common. One conclusion reached in the Dickens et al. paper that our results disagree with is their reported lack of NGC 288 giants that have mixed deeply. We find that approximately half of our NGC 288 sample have stars with low O, high Na, and high Al. While NGC 288 does not have many giants with [O/Fe] less than 0.0, it should be remembered that NGC 288 is likely to have a larger ab initio O abundance than NGC 362. Thus the extent of O depletion can be as great at a slightly higher [O/Fe] ratio. We suspect that Dickens et al. do not report NGC 288 giants undergoing deep mixing because of their small sample size, an unfortunate choice of giants, and because they did not report Na or Al abundances.

4.3. *Comparison with Other Globular Clusters*

To put the abundance patterns of NGC 288 and NGC 362 in context with other globular clusters, we will attempt to compare and contrast these two clusters with a few well-studied clusters of similar overall abundance. M4 ([Fe/H] = -1.18) and NGC 288 have very similar Na-O and Al-O anticorrelations (Ivans et al. 1999). M5 ([Fe/H] = -1.17) and NGC 362 have very similar Na-O and Al-O anticorrelations (Sneden et al. 1992; Shetrone 1996a). Neither NGC 288 nor NGC 362 have abundance

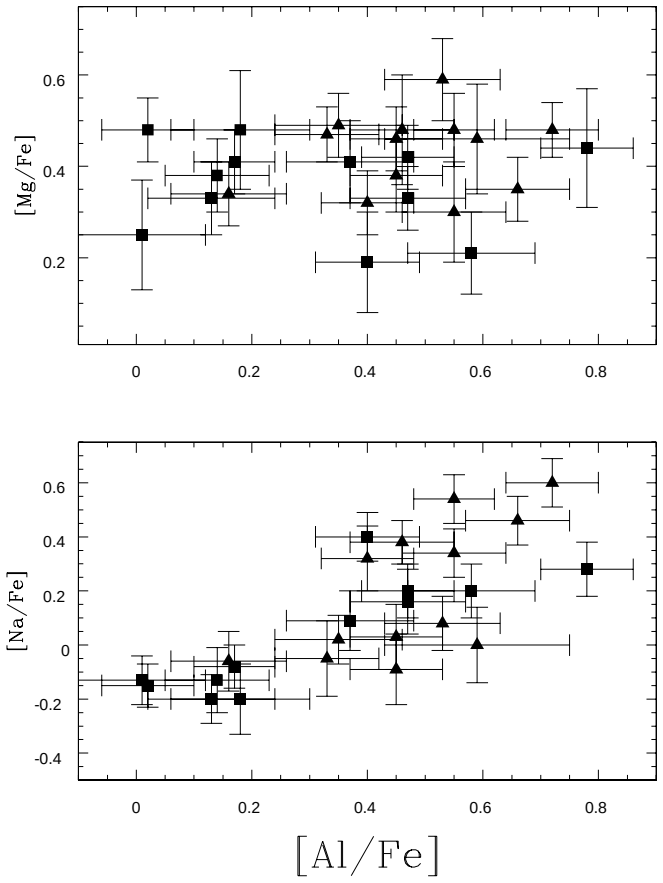


FIG. 3.—Abundances of the deep-mixing elements Mg and Na are compared with the Al abundances. The triangles represent the NGC 288 sample and the squares represent the NGC 362 sample. Error bars represent 1 σ errors.

patterns similar to the relatively more metal-poor cluster M13 ([Fe/H] = −1.6), which has extreme enhancements of Al and Na and extreme depletions of O (Kraft et al. 1997). NGC 3201 ([Fe/H] = −1.42) exhibits a different Na-O anticorrelation than both NGC 288 and NGC 362 and a

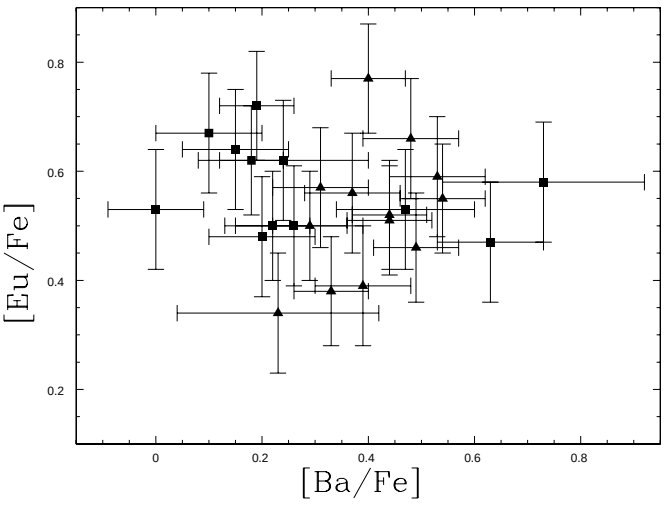


FIG. 4.—Ba abundances are compared with the Eu abundances. The triangles represent the NGC 288 sample and the squares represent the NGC 362 sample. Error bars represent 1 σ errors.

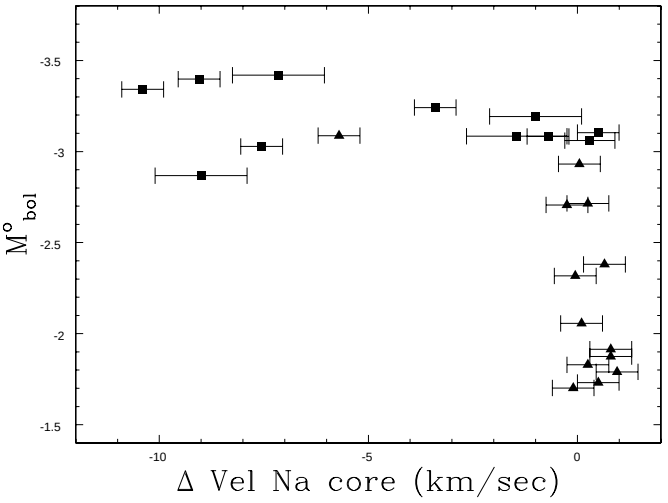


FIG. 5.—Bolometric magnitudes for the sample giants are plotted as a function of the Na D mass-loss indicator. The mass loss indicator is the velocity displacement in the core of the Na D lines. The triangles represent the NGC 288 sample and the squares represent the NGC 362 sample. Error bars represent 1 σ errors.

possible spread in [Al/Fe] at a given O abundance (Gonzalez & Wallerstein 1998). The samples of NGC 7006 (Kraft et al. 1998) and M3 (Kraft et al. 1992) are too small to determine if their Na-O and Al-O anticorrelations resemble NGC 362 or exhibit a different behavior. While NGC 362 and M5 have similar Eu and Ba abundances, M4 has a significantly larger Ba abundance than does NGC 288. For a recent discussion of the odd *s*-process abundance ratio of M4, see Ivans et al. (1999). In addition to the abundance similarities of NGC 288 and NGC 362 with M4 and M5, respectively, the clusters have similar microturbulent velocities at a given effective temperature. The microturbulent velocities of NGC 362 and M5 are systematically higher than those found in M4 and NGC 288.

4.4. *Mass Loss*

Table 5 lists the bolometric magnitudes, radial velocities, and mass-loss indicators. The bolometric corrections were computed by interpolating on the grids given in Vandenberg (1992). The core velocity was measured as the velocity difference of lowest point in a smoothed line profile from the rest velocity of the theoretical line core. This method is chosen to reduce the noise because of the very low flux found in the line cores. The Hα equivalent widths are given in milliangstroms. The blue and red Hα equivalent widths are defined as the flux, in milliangstroms, above the continuum on either the red wing or the blue wing of Hα. The velocity peak of the peak emission measured from the theoretical line center is listed next to the emission equivalent width. The Na D core velocities are the average of the Na D_1 and Na D_2 core velocities. There is a large range in Hα equivalent widths despite the narrow range in effective temperature. This range is caused by filling of the Hα line from chromospheric emission. The most extreme example of this emission is found in NGC 362 V2, which has Hα (and Hβ) completely in emission. This filling has the potential, if strong or broad enough, to cause the core of the Hα line to be displaced from the zero velocity position. Thus we do not give strong weight to the Hα core velocities as a mass-loss indicator.

TABLE 5

MASS-LOSS DATA FOR PROGRAM STARS

Star	M_{bol}	rv (km s^{-1})	Δrv (Na D)	EW (Hα)	Δrv (Hα)	Hα (red)	Peak Δrv	Hα (blue)	Peak Δrv
NGC 288									
531	−3.09	−40.7	−5.7	574	−2.3	61	35	6	−36
403	−2.93	−46.0	0.0	1097	−5.3	8	53	38	−45
274	−2.72	−40.5	0.2	1239	−1.5	0	...	0	...
20c.....	−2.71	−46.9	−0.3	1072	−4.6	0	...	14	−45
281	−2.38	−41.5	0.6	1192	−4.7	0	...	0	...
344	−2.32	−49.0	0.0	1116	−2.4	0	...	0	...
245	−2.06	−45.6	0.1	1085	−6.0	0	...	0	...
231	−1.83	−47.9	0.2	1161	0.8	0	...	0	...
338	−1.79	−49.2	0.9	1113	−6.5	0	...	0	...
297	−1.92	−43.3	0.8	1104	−5.0	0	...	0	...
351	−1.88	−47.0	0.8	1105	0.0	0	...	0	...
307	−1.70	−42.6	−0.1	1123	3.3	0	...	0	...
287	−1.73	−50.5	0.5	1170	2.4	0	...	0	...
NGC 362									
1401	−3.40	229.2	−9.1	748	−2.5	38	40	150	−39
2115	−3.42	224.1	−7.2	887	−3.0	20	42	23	−46
1423	−3.34	232.3	−10.4	767	−7.8	74	35	54	−45
V2	−3.24	223.9	−3.4	0	...	518	35	2178	−26
1334	−3.08	213.8	−0.7	1063	−1.6	0	...	19	−48
1441	−3.19	222.3	−1.0	1202	−4.1	0	...	0	...
2423	−3.08	220.6	−1.5	1082	−4.2	14	49	26	−44
1137	−3.10	223.5	0.5	1063	−1.3	0	...	22	−43
77.....	−3.03	221.6	−7.6	938	−6.3	31	41	16	−44
MB2.....	...	234.6	−10.0	869	−4.1	135	37	68	−49
2127	−2.87	222.6	−9.0	1059	−10.9	0	...	0	...
1159	−3.06	217.2	0.3	1214	0.9	0	...	0	...

Figure 5 displays the bolometric magnitudes against Na D core velocities. This figure is consistent with Shetrone (1994), who found that only giants brighter than −2.8 have blueshifted cores but not all giants brighter than this cut-off have blueshifted Na D cores. This is also consistent with the Belfast group's conclusions (Bates et al. 1993; Kemp & Bates 1995; Lyons et al. 1996). They found that giants brighter than log $(L/L_{\odot}) > 2.9$ (or $M_{bol} > -2.5$) have significant Na D core shifts. Both clusters have giants brighter than $M_{bol} > -2.5$ but our sample from NGC 288 only has two giants brighter than −2.8. Of these two giants, only one, NGC 288 531, has significant Na D core shifts. The core shifts in NGC 288 531 are not significantly larger than those found in the NGC 362 sample. The Hα emission found in NGC 288 and NGC 362 are not unusual in comparison to similar giants found in the Belfast group publications, with the exception of NGC 362 V2. The unusual nature of the NGC 362 V2 spectra (strong Li absorption, TiO, and Hα and Hβ emission) are discussed in Smith, Shetrone, & Keane (1999).

5. CONCLUSIONS

We find that the overall abundance of NGC 288 and NGC 362 is −1.39 and −1.33, respectively. These abundances are smaller than the results from previous high-resolution surveys and should be adopted for future photometric comparisons of these clusters. We find evidence for deep mixing taking place in both clusters in roughly equal proportions. However, if the sample of giants from Dickens et al. (1991) is included, then we suggest that NGC 288 has a lower percentage of mixed giants than does NGC 362. NGC 288 is found to have a slightly higher ab initio abundance of Ca, O, Na, and Al than NGC 362. Pilachowski, Sneden, & Kraft (1996) and Kraft et al. (1997) have shown that the halo field stars exhibit a range in O and Na abundances and attribute this to ab initio abundance differences and not deep mixing. Thus, it is not surprising that the unmixed cluster stars may show a range of ab initio Na, Al, and O abundance differences. The slightly higher ab initio abundance ratios in NGC 288 masks the extent of mixing taking place within its giants. When this fact is considered, the extent of mixing taking place within the two clusters is found to be approximately equal. The Al enhancements found in both clusters are consistent with enhancement caused by ^{25}Mg and ^{26}Mg depletions only and no ^{24}Mg depletions. We would predict that if the Mg isotopes are measured in NGC 288 and NGC 362, the stars with "normal" O, Na, and Al abundances will have "normal" halo Mg isotope ratios while stars with low O and high Al and Na abundances will have very low ^{25}Mg and ^{26}Mg abundances with respect to ^{24}Mg. Based on the deep-mixing hierarchy, there is no reason to suspect large or differential He surface enhancements because of deep mixing between the two clusters. Thus we conclude that difference in deep mixing cannot be the second parameter affecting horizontal branch morphology in these two clusters.

With the exception of the strange spectra of NGC 362 V2, the Hα emission of NGC 288 and NGC 362 are similar to each other and to the results found for other globular clusters reported in previous surveys. The core displacements of NGC 288 and NGC 362 are consistent with those reported previously in the literature. There is nothing unusual about the magnitude of mass loss found in either sample of giants.

Thus we conclude that there is not any unusual mass-loss activity in NGC 288 that might create an unusually blue horizontal branch.

If NGC 288 and NGC 362 have roughly the same abundance, roughly the same alpha enhancement ratios, roughly the same percentage of mixed stars, the same extent of deep mixing within those stars, and no extreme mass loss taking place on the giant branch, what second parameters remain? Further investigations into the following areas may provide further insight: ab initio He abundance, age differences, and the apparent difference between the number of giants near the tip of the giant branch between the two clusters. In addition, Buonanno et al. (1997) suggest "in general, the higher the cluster central density the higher is the relative number of stars populating the most blue region of its HB."

We would like to dedicate this work to Ed Langer, whose guidance, enthusiasm, and humor are sorely missed.

REFERENCES

Alcaino, G. 1975, A&AS, 21, 15
Armosky, B. J., Sneden, C., Langer, G. E., & Kraft, R. P. 1994, AJ, 108, 1364
Barbuy, B., Spite, F., & Spite, M. 1987, A&A, 178, 199
Bates, B., Kemp, S. N., & Montgomery, A. S. 1993, A&AS, 97, 937
Bolte, M. 1989, AJ, 97, 1688
Buonanno, R., Corsi, C., Bellazzini, M., Ferraro, F. R., & Fusi Pecci, F. 1997, AJ, 113, 706
Canterna, R., Ferrall, T., & Harris, W. E. 1983, ApJ, 258, 612
Catelan, M., & de Freitas Pacheco, J. A. 1996, A&A, 289, 394
Cavallo, R. M., Sweigart, A. V., & Bell, R. A. 1996, ApJ, 464, 79
———. 1998, ApJ, 492, 575
Costar, D., & Smith, H. A. 1988, AJ, 96, 1925
Croke, B. F. W. 1992, Ph.D. thesis, Univ. New South Wales
D'Cruz, N. L., Dorman, B., Rood, R. T., & O'Connell, R. W. 1996, ApJ, 466, 359
Dickens, R. J., Croke, B. F. W., Cannon, R. D., & Bell, R. A. 1991, Nature, 351, 212
Dupree, A. K., Hartman, E. F., & Avrett, A. K. 1984, ApJ, 281, 37
Dupree, A. K., Hartmann, L., Smith, G. H., Rodgers, A. W., Roberts, W. H., & Zucker, D. B. 1994, ApJ, 421, 542
Dupree, A. K., & Smith, G. H. 1995, AJ, 110, 405
Frogel, J. A., Persson, S. E., & Cohen, J. G. 1983, ApJS, 53, 713
Fusi Pecci, F., Bellazzini, M., Ferraro, F. R., Buonanno, R., & Corsi, C. E. 1996, in ASP Conf. Ser. 92, Formation of the Galactic Halo—Inside and Out, ed. H. L. Morrison & A. Sarajedini (San Francisco: ASP), 221
Gonzalez, G., & Wallerstein, G. 1998, AJ, 116, 765
Gratton, R. G. 1987, A&A, 179, 181
Gray, D. F. 1994, PASP, 106, 1248
Harris, W. E. 1982, ApJS, 50, 573
Ivans, I. I., Sneden, C., Kraft, R. P., Suntzeff, N. B., Smith, V. V., Langer, G. E., & Fulbright, J. P. 1999, AJ, 118, 1273
Kemp, S. N., & Bates, B. 1995, A&AS, 112, 513
Kraft, R. P., Sneden, C., Langer, G. E., & Prosser, C. F. 1992, AJ, 104, 645
Kraft, R. P., Sneden, C., Langer, G. E., & Shetrone, M. D. 1993, AJ, 106, 1490
Kraft, R. P., Sneden, C., Langer, G. E., Shetrone, M. D., & Bolte, M. 1995, AJ, 109, 2586
Kraft, R. P., Sneden, C., Smith, G. H., Shetrone, M. D., Langer, G. E., & Pilachowski, C. A. 1997, AJ, 113, 279
Kraft, R. P., Sneden, C., Smith, G. H., Shetrone, M. D., & Fulbright, J. 1998, AJ, 115, 1500
Langer, G. E., & Hoffman, R. 1995, PASP, 107, 1177
Langer, G. E., Hoffman, R., & Zaidins, C. S. 1997, PASP, 109, 244
Lee, Y. W., Demarque, P., & Zinn, R. 1994, ApJ, 423, 248
Lyons, M. A., Kemp, S. N., Bates, B., & Shaw, C. R. 1996, MNRAS, 280, 835
McWilliam, A., & Lambert, D. L. 1988, MNRAS, 230, 573
McWilliam, A., & Rich, R. M. 1994, ApJS, 91, 749
Olszewski, E. W., Canterna, R., & Harris, W. E. 1984, ApJ, 281, 158
Peterson, R. C. 1981, ApJ, 248, 31
Peterson, R. C., Rood, R. T., & Crocker, D. A. 1995, ApJ, 453, 214
Pilachowski, C. A., & Sneden, C. 1983, PASP, 95, 229
Pilachowski, C. A., Sneden, C., & Kraft, R. P. 1996, AJ, 111, 1689
Ridgway, S. T., Joyce, R. R., White, N. M., & Wing, R. F. 1980, ApJ, 235, 126
Rood, R. T. 1973, ApJ, 184, 815
Sandage, A., & Wildey, R. 1967, ApJ, 150, 469
Sarajedini, A., & Demarque, P. 1990, ApJ, 365, 219
Shetrone, M. D. 1994, PASP, 106, 161
———. 1996a, AJ, 112, 1517
———. 1996b, AJ, 112, 2639
Smith, G. H., & Dupree, A. K. 1988, AJ, 95, 1547
Smith, V. V., Shetrone, M. D., & Keane, M. J. 1999, ApJ, 516, 73
Sneden, C., Kraft, R. P., Prosser, C. F., & Langer, G. E. 1991, AJ, 102, 2001
———. 1992, AJ, 104, 2121
Stetson, P. B., VandenBerg, D. A., & Bolte, M. 1996, PASP, 108, 560
Tucholke, H. J. 1992, A&AS, 93, 311
Vandenberg, D. A. 1992, ApJ, 391, 685
Vandenberg, D. A., & Durrell, P. R. 1990, AJ, 99, 221
van den Bergh, S. 1967, AJ, 72, 70
Wallerstein, G., et al. 1997, Rev. Mod. Phys., 69, 995